Available online at www.sciencedirect.com
SCIENCE DIRECT®
Journal of Molecular Catalysis A: Chemical 212 (2004) 277–289
JOURNAL OF MOLECULAR CATALYSIS A: CHEMICAL
www.elsevier.com/locate/molcata

Surface Raman characterization of cinchonidine-modified platinum in ethanol: effects of liquid-phase concentration and co-adsorbed hydrogen

Rene J. LeBlanc, Wei Chu, Christopher T. Williams*

Department of Chemical Engineering, Swearingen Engineering Center, University of South Carolina, Columbia, SC 29208, USA

Received 24 August 2003; received in revised form 5 November 2003; accepted 7 November 2003

Abstract

Surface-enhanced Raman spectroscopy has been utilized to probe the adsorption of the chiral modifier cinchonidine on polycrystalline platinum. Surfaces were prepared by electrodeposition of ultrathin platinum films onto roughened gold, which provided stable and intense SERS activity for performing these studies. The vibrational properties of adsorbed cinchonidine on platinum in ethanol solutions at 25 °C have been probed in situ. Based on the appearance and trends in the strong ring breathing mode at 1357 cm^{-1}, the modifier is strongly and irreversibly adsorbed through the quinoline portion of cinchonidine by π-bonding with the Pt surface. Furthermore, analysis of both in-plane and out-of-plane vibrations suggests that the aromatic group of cinchonidine is tilted with respect to the surface. The degree of tilt appears to increase as concentration increases over the range of cinchonidine liquid-phase concentrations examined here (0.03–1.2 mM). The presence of an H-abstracted α-quinolyl species is also tentatively suggested by the appearance of a downshifted aromatic C=C stretching band not associated with adsorbed cinchonidine. These findings are largely consistent with what has been observed previously for cinchonidine adsorption on Pt from different solvents using in situ infrared spectroscopy. Addition of hydrogen into the system results in enhanced Raman scattering from adsorbed cinchonidine. Comparisons with SERS measurements of 10,11-dihydrocinchonidine adsorption in ethanol suggest that the H_2-induced changes likely result from hydrogenation of the vinyl group on cinchonidine. The data suggest a more flat orientation of this species, resulting from increased interaction of the aromatic ring structure with the surface. The results are consistent with kinetic studies of cinchonidine hydrogenation, which have implied much stronger adsorption of 10,11-dihydrocinchonidine as compared with cinchonidine.

Keywords: Surface-enhanced Raman spectroscopy (SERS); Cinchonidine; Enantioselective; Platinum

1. Introduction

The Orito reaction, which employs cinchona alkaloid modifiers to engender enantioselectivity in hydrogenation reactions catalyzed by transition metals, has drawn significant attention from the catalysis community over the years. This method is most effective for the asymmetric conversion of CO double bonds in α-ketoesters to the corresponding enantiopure lactates over platinum. Fig. 1 shows the hydrogenation of ethyl pyruvate, which is the most extensively studied of these reactions, as well as the molecular structure of the associated cinchonidine modifier. Cinchonidine is only needed in trace quantities to guide the reaction towards the desired product. In addition to this selectivity increase, the rate of reaction is also dramatically increased. Several review articles are available that have summarized the current state-of-the-art in this reaction [1–4].

Several kinetic models have been developed for this system based upon analysis of reaction experiments that have varied parameters such as temperature, H_2 pressure, modifier concentration, and solvent (see for example [5–8]). However, much less information is available regarding the specific surface interactions that engender the startling enantiomeric excesses (ee) and activities in this system. Wells and co-workers [9] made the first attempts at surface characterization by performing ultra-high vacuum (UHV) experiments. They examined the adsorption of cinchonidine on Pt(1 1 1) single crystal surfaces with LEED and XPS. They revealed that the cinchonidine does not form an ordered array on the surface and that it is most likely

* Corresponding author. Tel.: +1-803-777-0143; fax: +1-803-777-8265.
E-mail address: willia84@engr.sc.edu (C.T. Williams).

1381-1169/$ – see front matter © 2003 Elsevier B.V. All rights reserved.
doi:10.1016/j.molcata.2003.11.006

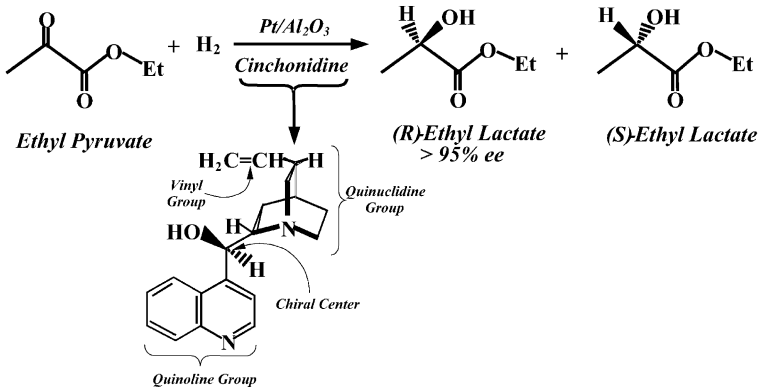

Fig. 1. Schematic of the enantioselective hydrogenation of ethyl pyruvate using a cinchonidine-modified platinum catalyst.

π-bonded to the surface through the quinoline group. A more recent UHV-based investigation has probed the related fragment molecules quinoline and lepidine on Pt(1 1 1) using XPS, NEXAFS, and STM [10]. It was determined that these molecules are anchored to the surface through a π-bond with the aromatic ring structure, with the degree of tilt increasing with increasing surface coverage.

It is only recently that in situ spectroscopic studies of cinchonidine adsorption on metals have been performed. Vibrational spectroscopic techniques such as attenuated total reflection infrared (ATR-IR) spectroscopy, reflection-absorption infrared spectroscopy (RAIRS), and surface-enhanced Raman spectroscopy (SERS) have allowed molecular-level observation of catalyst surfaces while varying different liquid-phase reaction parameters. For example, Ferri et al. [11,13] and Ferri and Bürgi [12] have examined cinchonidine adsorption on model supported Pt and Pd catalysts with ATR-IR. For most of their experiments, they utilized CH_2Cl_2 to reduce complications of interference from liquid-phase IR absorbance. The adsorption mode was found to be coverage dependant, with three different species observed: a "flat" π-bonded species at low coverage, a tilted quinoline N-bonded species at the highest coverage, and a tilted species at moderate coverage that has undergone α-H abstraction on the quinoline ring. Using RAIRS, Kubota and Zaera [14], Kubota et al. [15], and Ma et al. [16] have examined adsorption of cinchonidine on polycrystalline Pt surfaces from CCl_4 solutions, also revealing a flat orientation that tilts with respect to the surface at elevated liquid-phase concentrations.

In a recent communication, we presented a preliminary surface-enhanced Raman spectroscopic (SERS) study of adsorption of cinchonidine on polycrystalline Pt from ethanol [17]. The results appeared to be largely consistent with the previous spectroscopic findings described above. To perform SERS on platinum surfaces in the liquid phase, we used an approach pioneered by Zou and Weaver (for an overview see [18], and references therein). In this method, a thin film of a transition metal (in this case Pt) is electrochemically deposited onto a SERS-active gold substrate. The electromagnetic Raman enhancement from the gold penetrates through the Pt, yielding intense Raman scattering from molecules adsorbed on the overlayer. This approach has been used to examine both gas-phase catalytic and electrochemical systems [19,20]. In the case of surfaces in the liquid phase, the use of confocal Raman microscopy is additionally helpful due to the fact that a large fraction of the bulk liquid signal can be rejected.

In this study, we present a comprehensive SERS investigation of cinchonidine adsorption on polycrystalline platinum from ethanolic solutions at 25 °C. Vibrational band assignments for bulk and adsorbed cinchonidine are made based on information available in the literature as well as density functional theory (DFT) calculations. The effects of cinchonidine liquid-phase concentration on surface coverage and adsorption orientation are examined in light of these assignments. Furthermore, the effects of co-adsorbed hydrogen on the adsorption of cinchonidine are studied. Finally, the adsorption 10,11-dihydrocinchonidine on Pt is compared with cinchonidine adsorption both in the presence and absence of hydrogen.

2. Experimental

2.1. Materials

Cinchonidine (Fluka, 98%), dihydrocinchonidine (Merck), ethanol (Aldrich, 99.5%), dihydrogen hexachloroplatinate (Premion, 99.95%), potassium chloride (J.T. Baker), sodium phosphate (Fisher, 99.1%), and hydrogen gas (National Welders, UHP) were all used as supplied. Water was purified via a Barnstead B-pure initial low inorganic filtration followed by a Milipore low organic filtration to ca. 18 MegaOhm/cm resistance.

2.2. SERS-active platinum preparation

SERS-active Pt substrates consist of thin Pt overlayers deposited on roughened gold electrodes. Gold electrodes

were prepared using gold wire (Premion, 99.999%, 1.4 mm) and a Teflon rod (DuPont). The rod is bored with a concentric hole (ca. 1 mm) and a length (ca. 2 mm) of gold wire is press fit into one end. The electrical contact is formed from a stainless steel screw fit into the opposite end of the bored hole. These surfaces were then polished in stages down to 0.05 μm alumina powder. Electrochemical treatments were then performed using an EG&G M273A potentiostat, with potentials referenced to a saturated calomel electrode (SCE). The mirror-finished electrodes were first electrochemically roughened in a deaerated aqueous 0.1 M KCl solution to induce SERS activity. The electrode is roughened by holding the potential of the gold surface at −0.3 V for 30 s, sweeping the voltage to 1.2 V at 500 mV/s, holding at 1.2 V for 1.1 s, and then sweeping back to –0.3 V. This cycle is repeated 25 times to achieve optimal SERS activity [21]. Platinum is plated from a deaerated aqueous solution containing 5 mM H_2PtCl_6 and 0.7 M Na_2PO_4 by holding at a constant current of 15 μA for 90 s [18].

2.3. Raman instrumentation and spectral acquisition

A LabRam confocal Raman spectrometer (JY Horiba) is used for all SERS measurements. The spectrometer is equipped with a liquid-nitrogen cooled, charged coupled device (CCD) detector, and a HeNe (632.817 nm) laser for excitation. A robotic stage is used to move the sample in micrometer increments under the laser, thus allowing spectra to be obtained from multiple points in a controlled fashion. It is well known that the surface-enhancement on a roughened gold surface will vary from point to point [22,23], depending on roughness heterogeneity and any “hot” spots (i.e., roughness features exhibiting unusually large Raman enhancement). Thus, obtaining Raman spectra from only one spot (or even a few spots) on the surface may lead to results that are not representative of the entire surface. As a result, the Raman spectra reported here were acquired by averaging spectra obtained from an array of points on the surface. For example, rather than acquiring a spectrum from one spot on the surface for 100 s, we would obtain a spectrum from each of 100 different spots using 1 s acquisition per spot. These spectra are then averaged to produce the representative surface spectra. A typical measurement involves an average of between 100 and 400 spectra, each acquired with 1 s integration time. Prior to fitting each averaged spectrum, a baseline correction was performed by linearly connecting four points. These consisted of the spectral end points of the plot, plus two internal points that

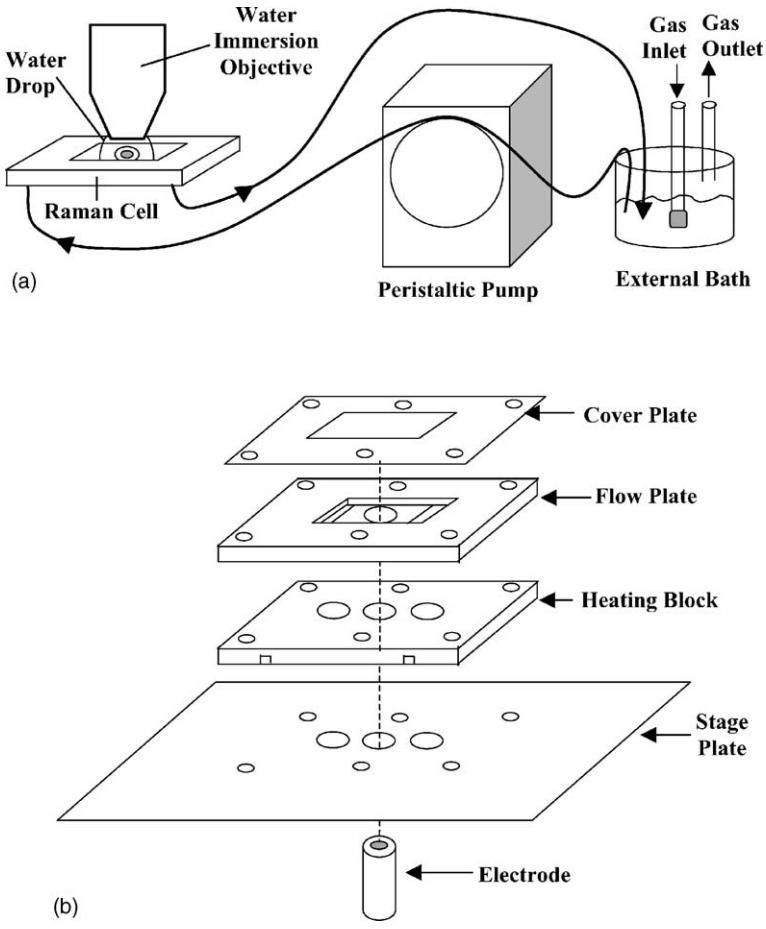

Fig. 2. Schematic of the liquid flow cell used to obtain in situ Raman spectra of platinum surfaces. See text for details.

were chosen so that the baseline correction would not affect the shapes or intensities of any observed peaks. Peak fitting of the Raman data was accomplished using PeakSolve, a commercial windows-based software package.

2.4. Liquid flow cell

A liquid flow cell (designed in house) allows the Olympus microscope stage of the LabRam instrument to image the flat electrode surface under flow conditions. Fig. 2 shows an expanded view of the parts involved in the flow cell. The flow cell itself is assembled in layers. The lowest layer on the diagram is a base plate, which allows the spectrometer's robotic stage to reproducibly move the cell as requested by the control software. The next layer is an optional heating block and associated gasketing. The gasket between the base plate and the heating block is for electrical insulation. This block has been machined to accept a 0.5 cm heating wire in a single-path serpentine channel. The thin plate above the heating block is a compression O-ring block. This plate is slightly thinner than the associated Viton O-rings, forcing the O-rings to compress around the tubes and electrode, forming a liquid-tight seal. The flow plate is a solid 340 stainless steel block that has been designed to flow the liquid stream past the electrode surface. The flow channel width and length has been designed to reduce turbulent flow (which can cause problems with optical focus and reproducibility) in the region between the surface and the optical window. A quartz cover slip (VWR, 25 mm × 50 mm) is used as the optical window and is sealed in place by a top cover plate.

Cinchonidine was found to be very difficult to remove from the cell by simple washing with detergent followed by rinsing with water and ethanol. Treatment in this fashion would typically result in trace quantities of cinchonidine remaining, which could then often be detected on fresh SERS surfaces upon exposure to ethanol in the flow cell. As a result, the following cleaning procedure was used. The flow cell was baked at 300 °C in air for 2 h followed by washing with an acidic detergent to remove any remaining carbonaceous species. The cell was then thoroughly rinsed with deionized water, followed by a final rinse in ethanol before introduction of a fresh SERS-active surface.

3. Results and discussion

3.1. Vibrational band assignments for cinchonidine

The relative complexity of the cinchonidine molecule makes interpretation of vibrational data (both bulk and surface derived) a considerable challenge. Cinchonidine has 126 normal modes of vibration and, since the molecule is chiral, all of these vibrations are in principle both infrared and Raman active. It is, therefore, perhaps unsurprising that a full set of vibrational band assignments of this molecule

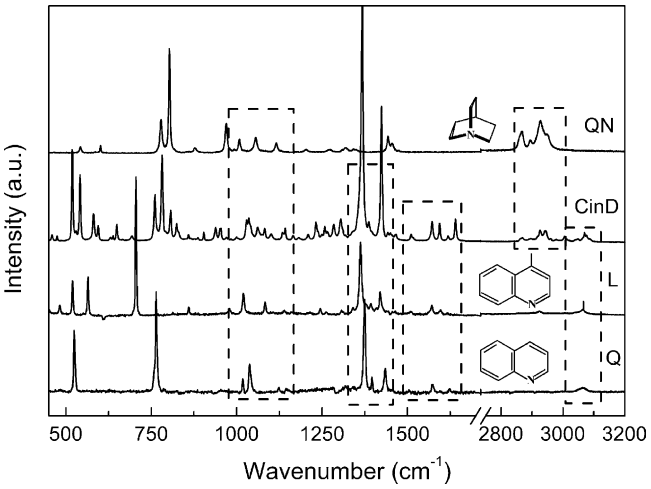

Fig. 3. Normal Raman spectra for bulk quinoline (Q), lepidine (L), cinchonidine (CinD), and quinuclidine (QN). The dashed boxes indicate the similarities between the spectra.

was not available in the literature. As a result, prior to examining the SER spectra for this system, it was necessary to assign some of the key vibrational modes of cinchonidine. This band assignment process is the subject of a forthcoming study that utilizes both DFT and Hartree–Fock computational approaches for frequency calculations [24]. Nevertheless, for the purposes of the ensuing discussion we present a brief summary of this band assignment procedure here.

The first step was to assign as many cinchonidine peaks as possible via consultation of characteristic frequency tables [25,26] and reported vibrational band assignments [12,14,15,27]. Furthermore, general comparisons were made with the spectra of quinoline, lepidine, and quinuclidine, which are fragments of cinchonidine. For example, the Raman spectra of these molecules are shown in Fig. 3, along with the structure of each. Comparing the spectra, one can clearly see similarities between frequency regions (indicated by the dashed boxes). Due to the large number of overlapping peaks in cinchonidine, the Raman and infrared spectra of this molecule were deconvoluted by fitting each entire spectrum with a series of individual peaks. By combining fitted peak information from both Raman and infrared data, a complete list of vibrational peaks (as well as harmonics and combination bands) was generated. A list of the peak frequencies and associated line strengths that are relevant to the present work is presented in Table 1.

Once the initial band assignments were completed, DFT calculations were performed using the B3PW91 "hybrid" approach with several different basis sets. The software package used was Gaussian 98W [28] and visualization of the vibrational modes was accomplished using MacMolPlt [29]. The structure of solid cinchonidine has been clearly identified by X-ray diffraction [30] and is shown in Fig. 4. This structure is the same as the A2 structure reported by Margitfalvi and Tfirst in a molecular modeling study of

Table 1
Vibrational band assignments for cinchonidine and cinchonidine/Pt in ethanol

Solid cinchonidine[a]			On Pt	Description of vibrational mode[m]
Raman (cm^{-1})	IR (cm^{-1})	Calc.[b] (cm^{-1})	SERS[c] (cm^{-1})	
758 (m)	nd	759	784	Q C–H o.p. wag + small QN def[e,f]
779 (m)	nd	777	–	Q C–H o.p. wag + small QN def[e,f,g]
1163 (vw)	1163 (w)	1164	1154	QB C–H i.p. bend. + QN CH_2 wag/rock[f,g]
1207 (vw)	1207 (w)	1213	1209	QN CH_2 tors and wag + Q CH IP bend[e,g]
1281 (w)	1277 (w)	1287	1296	Vinyl C–H rock[d]
nd	1298 (w)	1294	–	Vinyl CH bend + QN CH wag[d]
1302 (w)	1306 (w)	1299		QN CH and CH_2 wag[e]
1326 (vw)	1326 (w)	1320	1328	QN CH_2 wag[e]
1336 (vw)	1336 (w)	1321	–	QN CH wag + Q CNC and CCC A str[e]
1366 (vs)	1366 (w)	1374	1357	Q ring str and CH i.p. bend + QN CH wag[f,g,h,i]
1383 (w)	1383 (w)	1384	–	Q ring str and CH i.p. bend[f,g,h,i,j,k]
1508 (vw)	1508 (m)	1508	1512	Q i.p. ring def + small Q C–H i.p. bend[f,g,h,i,j,k]
–	–	–	1543	Q C=C ring stretch of α-quinolyl species[l]
1569 (w)	1569 (m)	1559	1572	Q i.p. ring def + small Q C–H i.p. bend[f,g,h,i,j,k]
1591 (w)	1591 (m)	1592	1587	Q i.p. ring def + small Q C–H i.p. bend[f,g,h,i,j,k]
1617 (vw)	1617 (w)	1623	1613	QB i.p. ring def + small Q C–H i.p. bend[f,g,h,i,j,k]
3074 (vw)	3074 (w)	3082	3071	Vinyl A C–H str[d]
3086 (vw)	3086 (vw)	3086	3089	QP C–H str

[a] The following letters describe the strengths of vibrational bands relative to the most intense band in the spectrum: vw: <5%, w: 6–25%, m: 25–75%, s: 75–95%, vs: 96–100%, nd: not detected.
[b] DFT calculations performed using the B3PW91 method with the LANL2DZ basis set. See text for details.
[c] Peaks observed in the SER spectra for Pt in 1.2 mM cinchonidine in ethanol at 25 °C (cf. Fig. 5).
[d] Consistent with characteristic frequency tables in (see [23,24]).
[e] Supported by comparison with bulk Raman spectrum of quinuclidine (cf. Fig. 3).
[f] Supported by comparison with bulk Raman spectra of lepidine and quinoline (cf. Fig. 3).
[g] Consistent with published band assignments for 2,2′-biquinoline (see [61]).
[h] Consistent with published band assignments for lepidine (see [62]).
[i] Consistent with published band assignments for monosubstituted quinolines (see [63]).
[j] Consistent with published band assignments for cinchonine (see [64]).
[k] Consistent with published band assignments for cinchonidine (see [12]).
[l] Surface decomposition product of cinchonidine. See text for details.
[m] Approximate cinchonidine mode description using the following notation: Q: quinoline group, QB: benzene part of quinoline group, QP: pyridine part of quinoline group, QN: quinuclidine group, i.p.: in-plane, o.p.: out-of-plane, A: asymmetric, def: deformation, str: stetching, bend: bending, tors: torsion, wag: wagging, rock: rocking.

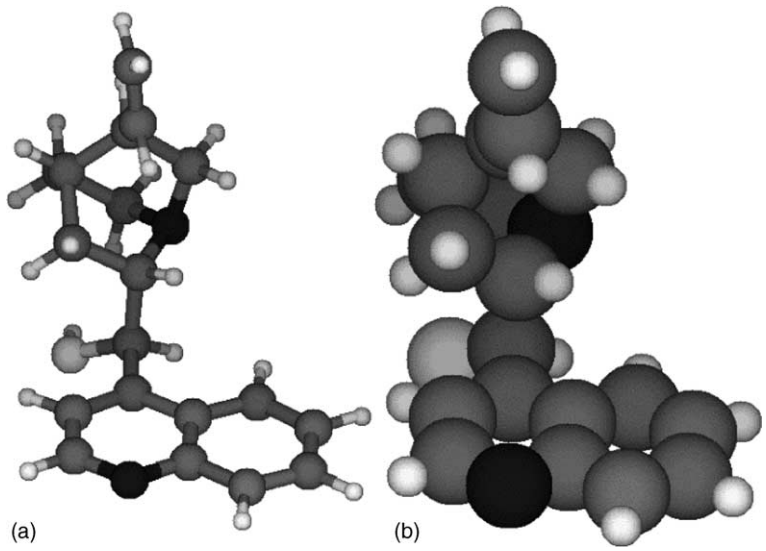

Fig. 4. The structure of solid cinchonidine used for calculations of vibrational frequencies, with both: (a) “ball and stick” and (b) connected sphere representations shown. See text for details regarding this structure.

cinchonidine [31]. It is one of the six so-called "open" conformers, corresponding to structures for which the tertiary nitrogen of the quinuclidine group points away from the aromatic quinoline ring. We have, therefore, used this structure as the basis for our DFT calculations. Following geometry optimization of the A2 structure, vibrational frequencies were calculated in order to compare with experimentally obtained frequencies. While different levels of theory have been employed for this system [24], Table 1 is limited here to frequencies calculated using B3PW91 method [32–34] with the LANL2DZ basis set [35–37]. It is well known that DFT methods overestimate the frequency of molecular modes, typically by around 1–5% [38]. Using readily assigned vinyl and quinoline ring modes, we developed frequency scale factors for the regions below (0.9657) and above (0.9431) 1800 cm^{-1}, as has been previously suggested by Halls et al. [39–41] and Palafox [42]. As can be seen in Table 1, the calculated frequencies after the scaling procedure are in excellent agreement with the experimental frequencies.

3.2. SER spectra of cinchonidine on platinum in ethanol

Armed with several vibrational band assignments for cinchonidine, SER spectra were acquired for cinchonidine adsorbed on Pt in ethanol. This was the subject of a previous preliminary communication [17], and here we expand the discussion regarding the spectral interpretation. Due to the complexity of the spectra that were obtained, a deconvolution procedure was required to extract the desired SER signal from that of other signals in the system. For example, the bottom trace of Fig. 5 shows an in situ SER spectrum obtained from platinum immersed in ethanol containing 1.2 mM cinchonidine. The spectrum is complicated and contains many overlapping peaks from a variety of sources. The peaks at 882, 1051, 1095, 1276, and 1456 cm^{-1} can be readily assigned to Raman scattering from bulk ethanol solvent. The presence of these peaks is expected, as the confocal collection optics cannot eliminate bulk phase scattering completely. Since we have not observed any peaks associated with adsorbed ethanol when the modifier is absent from the solution, most of the remaining peaks in the spectrum are assumed to be from the adsorbed cinchonidine. The exceptions are the broad humps that lay beneath the peaks between 1200 and 1700 cm^{-1}. These features are associated with trace amounts of carbonaceous impurities on the surface, as noted in many SERS investigations (see for example [23]). The actual peak positions are typically at around 1580 and 1340 cm^{-1}, and are representative of graphitic and amorphous/disordered carbon, respectively [43].

Before fitting could proceed, the peaks used to model liquid ethanol and carbonaceous impurities were determined. This was accomplished by fitting the Raman spectra obtained from pure ethanol (not shown), as well as from Pt in pure ethanol [17], for which the only observed surface peaks arise from carbonaceous impurities. The resulting peak parameters for these species were then used when fitting the SER spectra in the presence of cinchonidine. Initial inputs for cinchonidine-related peaks were chosen based on the shape of the overall spectra and examination of residuals after subtraction of ethanol and surface carbon contributions. The peaks from liquid-phase ethanol and adsorbed cinchonidine were modeled by pure Lorentzian lineshapes, while the carbonaceous impurities were modeled by a hybrid Lorentzian/Gaussian function. Several constraints were placed on the peak parameters during the fitting routine within a data set. While the intensities of the ethanol peaks

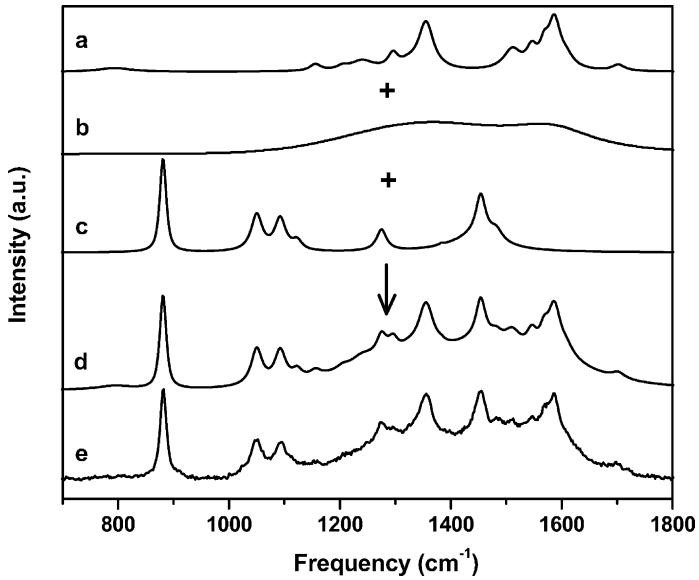

Fig. 5. Deconvoluted spectra of: (a) adsorbed cinchonidine, (b) surface carbonaceous impurities, and (c) liquid-phase ethanol obtained by curve-fitting an in situ SER spectrum of platinum in 1.2 mM cinchonidine in ethanol. The overall fitted Trace (d) provides an excellent fit of the experimental data (e). See text for details of the curve fitting procedure.

were allowed to vary, their positions, full widths at half maximum (FWHM), and relative sizes to each other were kept fixed. The same constraints were placed on the carbon peak parameters, except that the intensities were allowed to vary. Finally, the intensities of the adsorbed cinchonidine peaks were allowed to vary from fit to fit while keeping other parameters constant.

Fig. 5 provides an example of typical results of this fitting procedure for the case of cinchonidine adsorbed onto Pt in a 1.2 mM ethanolic solution. The peaks that are obtained through the fit have been recombined to show the fitted pure component spectra for adsorbed cinchonidine (Trace a), surface carbon (Trace b), and liquid ethanol (Trace c). Adding these three traces together yields the overall fit (Trace d), which is in excellent agreement with the experimental spectrum (Trace e). In this way, the trends in the surface cinchonidine peaks could be reliably extracted for a series of spectra. The initial fit was always first performed on the highest concentration level so as to get the most accurate representation of all of the possible peaks. The resulting fitted peak parameters were then often used as initial inputs for the next lowest cinchonidine concentration. This procedure would then be repeated until the entire set of spectra was fitted.

The extracted peaks for adsorbed cinchonidine were assigned by comparison with the set of assigned peaks for solid cinchonidine. The band assignments for these surface peaks are listed in Table 1. The most prominent spectral feature is the large SERS peak at 1357 cm^{-1}, which is assigned to a quinoline ring stretching mode of cinchonidine adsorbed on Pt. The specific stretching involves the carbons located at the junction between the pyridine and benzene parts of the quinoline group. It is not surprising that this feature should be observed in the SER spectra, since it is the strongest vibration in the bulk Raman spectrum. The presence of this feature provides two clues as to the mode of adsorption. First, the peak is broadened significantly from its solid-phase value, increasing from ca. 6 to ca. 30 cm^{-1}. Second, the peak is downshifted ca. 10 cm^{-1} upon cinchonidine adsorption. Both observations suggest that the quinoline group of the cinchonidine is π-bonded to the Pt surface. Indeed, the result is consistent with SERS measurements of quinoline on Pt (data not shown), which reveal a similar broadening and downshift in the associated ring-stretching mode. This strong interaction of the aromatic rings with the surface is consistent with what has been observed in other studies of this system [9–15]. While it is unlikely that the intensity of this band varies exactly linearly with surface coverage (especially at high values, see [44,45]), we have nevertheless used this band to track the presence and amount of this species under a range of liquid-phase concentrations.

By examining the ratios of peaks within the SER spectra, a qualitative determination of the molecular orientation of the quinoline group is possible [46]. We take here the example of adsorption onto Pt from a liquid-phase containing 1.2 mM cinchonidine (Fig. 5). While the strong interaction of the aromatic ring with the surface would suggest a largely flat orientation, analysis of the SERS spectra suggests a significant tilt with respect to the surface. This is indicated by consideration of the relative strengths of out-of-plane and in-plane vibrations within the quinoline ring structure. Unfortunately, there are not many pure out-of-plane aromatic vibrations in solid cinchonidine (i.e., most also include a contribution from the quinuclidine portion of the molecule), and many such peaks are very weak Raman scatterers. Nevertheless, a broad feature in the SER spectra at ca. 784 cm^{-1} arises from a convolution of several largely out-of-plane vibrations (758 and 779 in the bulk Raman, see Table 1). These vibrations arise from out-of-plane C–H stretching on the aromatic rings. There are several in-plane vibrations to choose from in the SER spectra, most notably the three peaks at 1512, 1572, and 1587 cm^{-1}, corresponding to the aromatic in-plane C=C stretching modes at 1514, 1569, and 1591 cm^{-1}, respectively. When compared with the relative intensities of these bands in the normal Raman spectrum of cinchonidine (cf. Fig. 3), it is clear from the SER spectrum in Fig. 5 that the set of in-plane vibrations are enhanced considerably more than the out-of-plane vibrations. Thus, at this concentration it appears that the quinoline group is significantly tilted with respect to the Pt surface. Such SERS selection rule arguments are well documented and have been successfully used to analyze surface orientation of molecules having extended aromatic structure [47–49]. Evidence for a tilt in the aromatic ring is also provided by the observation of a SERS peak at ca. 3089 cm^{-1} (not shown in Fig. 5), corresponding to an in-plane C–H stretch of one of the two hydrogen atoms on the pyridine half of the quinoline group. Other cinchonidine C–H stretching vibrations are obscured by large ethanol-related peaks.

Ferri and Bürgi [12] have reported the presence of an "α-quinolyl" species during ATR-IR studies of cinchonidine adsorption onto a model supported Pt catalyst. This species is similar to the α-pyridyl species that has been observed during pyridine adsorption on transition metals [50,51]. The adsorbate is formed when the H in the alpha position with respect to N in the quinoline group is abstracted onto the surface. The adsorption configuration is through the nitrogen and adjacent carbon, and results in a near perpendicular orientation with respect to the surface. In their IR study, Ferri and Bürgi observed a prominent surface peak at 1530 cm^{-1}, which they attributed to the downshifted quinoline C=C stretching mode of the α-quinolyl. In the present SER spectra of adsorbed cinchonidine (Fig. 5), a prominent SERS peak is observed at 1543 cm^{-1} that does not appear to correspond to any observable peak in cinchonidine. We, therefore, tentatively assign this feature to an α-quinolyl species co-adsorbed with undissociated cinchonidine. Interestingly, recent electrochemical SERS investigations [52,53] of pyridine adsorption on Pt in both aqueous and non-aqueous (i.e., acetonitrile) solutions have not detected the presence of α-pyridyl species. It is likely that solvent and the presence of electrolytes have a significant effect on the formation of this species, especially in the case of strong solvent

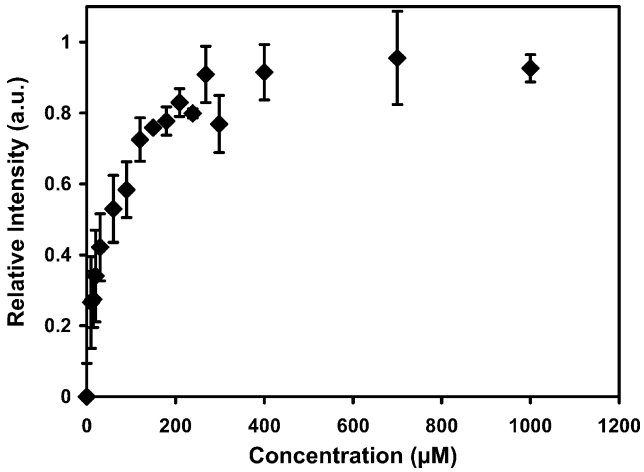

Fig. 6. Relative intensity of the 1357 cm^{-1} in-plane ring stretching vibration of adsorbed cinchonidine on Pt plotted as a function of liquid-phase cinchonidine concentration in ethanol. The intensity scale is normalized to the maximum intensity obtained at the highest concentrations.

adsorption (as might be occurring with acetonitrile). We are presently examining the adsorption behavior of cinchonidine in different solvents in order to explore this issue.

3.3. Effects of liquid-phase cinchonidine concentration on cinchonidine adsorption

Concentration-dependant experiments were conducted by starting with a fresh SERS active Pt film electrode in flowing ethanol. After the system was allowed to equilibrate, cinchonidine was added to the ethanol reservoir via injections of stock solution (0.01 M cinchonidine in ethanol) to increase the concentration in the system. The cinchonidine was added into the solution using ca. 0.060 ml increments until the concentration reached 1 mM, at which point larger injections were used to bring the concentration to 10 mM. Fig. 6 shows the effect of increasing solution-phase cinchonidine concentration on the intensity of the 1357 cm^{-1} peak of adsorbed cinchonidine on platinum. All intensities are normalized against the maximum intensity observed. Only the data obtained up to 1 mM concentration are shown, since higher concentrations did not result in any further changes in the SER spectra.

It is evident from Fig. 6 that even at the lowest concentrations there is some adsorption on the surface. The band increases markedly until a concentration of approximately 0.300 mM. However, as the liquid-phase concentration is increased one order of magnitude further the intensity remains unchanged. It is important to note that the intensities of the carbon peaks remain largely unchanged over this whole concentration range, suggesting that the adsorbed carbonaceous impurities are not displaced or formed with adsorption of cinchonidine. Removing the cinchonidine from the solution by flushing the flow cell with pure ethanol resulted in no observable change in the SERS intensities for adsorbed cinchonidine. This suggests that the cinchonidine is strongly and irreversibly adsorbed on the surface in ethanol. In addition to being in harmony with recent FTIR studies [11–15], this behavior is consistent with the reported success of the "ex situ" modification method for this catalytic system [1]. In this approach, cinchonidine is adsorbed on the catalyst in a separate solution, filtered, and then transferred into the reactant mixture. The ability of the modifier to remain irreversibly adsorbed on the surface during this procedure is therefore critical.

While it is clear from Fig. 6 that full coverage of cinchonidine has been reached at the highest concentrations, the exact point of surface saturation is difficult to discern. While SERS intensity and surface concentration have been shown to vary in a largely linear fashion at low to moderate coverages, it has been demonstrated that at high coverage the relationship is non-linear [44,45]. For example, Lipkowski and co-workers [44] have shown such a non-linear behavior for the aromatic molecule pyrazine on polycrystalline Au. They observed that the SERS intensity began to level off above about two thirds of a monolayer. As such, the value of 0.300 mM quoted above is likely a lower bound on the liquid-phase concentration that provides maximum coverage.

One of the hallmarks of the cinchonidine-mediated hydrogenation reaction on Pt is that the enantioselectivity changes as the amount of cinchonidine in the system is varied. From kinetic investigations (see for example [54]), it has been found that the optimal ratio lies at around 1 cinchonidine molecule per 10 exposed platinum atoms in the system. These changes have been proposed to arise through a combination of coverage and orientation effects. It is, therefore, useful to examine the effect of cinchonidine concentration on the surface orientation. Fig. 7 shows the intensity ratio of the 1587 cm^{-1} in-plane aromatic C=C stretching mode to the 784 cm^{-1} out-of-plane C–H wagging mode plotted

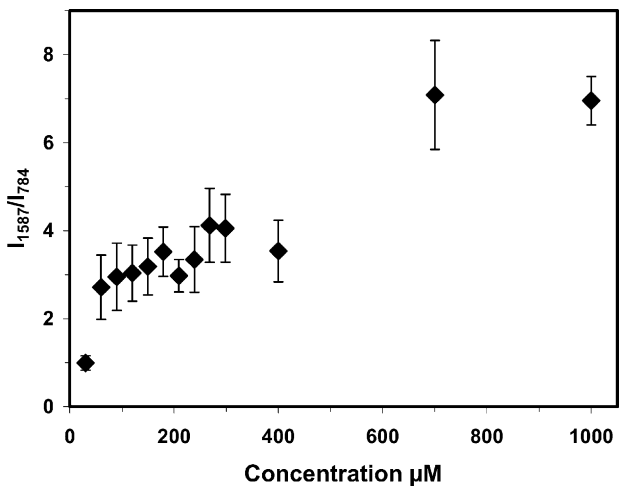

Fig. 7. Ratio of the 1587 cm^{-1} band intensity to the 784 cm^{-1} band intensity of adsorbed cinchonidine on Pt plotted as a function of liquid-phase cinchonidine concentration in ethanol.

versus the liquid-phase cinchonidine concentration in ethanol. The increasing trend in the ratio with increasing coverage suggests an increase in the tilt of the aromatic group with respect to the surface. Similar trends are also observed in the ratios of the other in-plane vibrations to the out-of-plane mode. While these data show that cinchonidine is tilted on the surface even at the lowest solution-phase concentration examined here (0.030 mM), extrapolation of the trend suggests that the quinoline group would continue to flatten as the coverage is lowered further. Measurement of the absolute surface coverage in these experiments is very difficult, and therefore, it is not possible to correlate this SERS data quantitatively with previously reported optimal cinchonidine coverages. However, recent electrochemical studies [55] show that the coverage of cinchonidine on Pt can be estimated using cyclic voltammetric measurements in acidic media. We are presently pursuing this approach in our laboratory. Nevertheless, the changes in orientation with cinchonidine coverage are consistent with the idea that orientation is a key parameter that influences the optimum Pt/cinchonidine ratio for enantioselective hydrogenation.

3.4. Effect of hydrogen on cinchonidine adsorption

Having probed the concentration-dependant adsorption of cinchonidine on Pt, the next step was to examine the effect of co-adsorbed hydrogen on this modifier. It is well known that cinchonidine is hydrogenated first at its vinyl group to form 10,11-dihydrocinchonidine, followed by deeper hydrogenation on the quinoline group [1,56]. It was therefore expected that solution-phase H_2 would have a pronounced effect on adsorbed cinchonidine. The following protocol was used to introduce hydrogen into the system. The Pt-surface was first exposed to pure ethanol, followed by introduction of cinchonidine to reach the desired liquid-phase concentration. After a steady SERS response was achieved, hydrogen was sparged through the solution. Fig. 8a shows SER spectra obtained for a Pt surface in 0.120 mM cinchonidine both before (bottom) and after (top) hydrogen sparging. The introduction of hydrogen is seen to have a dramatic effect on the SERS response. The intensities of the SERS bands associated with cinchonidine are seen to increase to varying extents, with the most pronounced effect observed for the 1357 cm^{-1} band. Fig. 8b shows the relative intensity of the 1357 cm^{-1} band as a function of solution-phase cinchonidine concentration for the case when hydrogen is present in solution. For comparison, the data for cinchonidine adsorption in the absence of H_2 (cf. Fig. 6) is also included. All the data are normalized to the average intensity observed at full coverage without H_2. The introduction of H_2 affects the SERS response over the entire range of concentrations in three ways. First, the relative intensity of the 1357 cm^{-1} band increases (in general) to 3–5 times those observed at the same concentration without hydrogen. Second, the liquid-phase concentration required to reach surface saturation (ca. 0.030 mM) is one order of magnitude lower with H_2 present. The third difference is that the intensity of the 784 cm^{-1} out-of-plane vibration has increased to a greater extent than the in-plane modes (e.g., 1587 cm^{-1}).

Before interpreting these results as they may relate to heterogeneous catalytic hydrogenation of cinchonidine, some other possible causes for the signal enhancement are considered. One possibility is that, if the morphology of the Pt surface changed dramatically with H_2 adsorption, the degree of enhancement might change. This in turn could cause the increased surface cinchonidine signals that are observed. Another explanation might be that the H_2 is cleaning the Pt surface of either oxygen or carbonaceous impurities, thus allowing more cinchonidine to adsorb. Fig. 9 shows the results of a stepwise experiment that was performed to probe whether the observed changes are caused by H_2-induced restructuring or cleaning. A fresh Pt surface was first prepared and immersed in ethanol (Spectrum a). In addition to the peaks from bulk ethanol and surface carbon, a peak is observed at around 2090 cm^{-1} that arises from adsorbed atomic hydrogen. The source of this species appears to be from the dissociation of ethanol. The peak is not present directly after the electrochemical treatment. This assignment is based on comparisons with previous SERS [57] and SFS [58,59] studies of hydrogen adsorption on Pt. Upon introduction of H_2 (Spectrum b), this peak downshifts to 2070 cm^{-1} and grows in intensity. Concurrent with this increased H adsorption is a drop in the signals associated with carbonaceous impurities. This is likely the result of displacement of these species from SERS sites by H atoms. The adsorbed H peak upshifts slightly and decreases in intensity when hydrogen is purged from the solution with He (Spectrum c). Following this pretreatment, the cinchonidine concentration was stepped to 0.240 mM, resulting in the appearance of the expected surface peaks (Spectrum d). However, the signal enhancement for adsorbed cinchonidine is not observed until the H_2 is again introduced into the solution (Spectrum e). Furthermore, analysis of the Spectra d and e reveals that the broad carbon bands that make up the mid-frequency background (cf. Fig. 5) remain largely unchanged during the second addition of hydrogen. This leads us to conclude that the observed changes in the SER spectra with H_2 in solution are not the result of either a SERS activity change or a surface cleaning effect.

The likely cause of this enhancement is thus an interaction or reaction between hydrogen and adsorbed cinchonidine. As already mentioned, one definite reaction that is known to occur is the hydrogenation of the vinyl group to form 10,11-dihydrocinchonidine (DHCD). Such a reaction might induce a change in orientation with respect to the surface that would alter the Raman response. To test this theory, the adsorption of DHCD from an ethanolic solution was examined. Fig. 10 shows the typical SER spectra for platinum in a 0.240 mM solution of DHCD before (bottom spectrum) and after (middle spectrum) introduction of hydrogen. The first thing to note is that the SER spectrum of DHCD on Pt is very similar to that of cinchonidine. The fact that no new

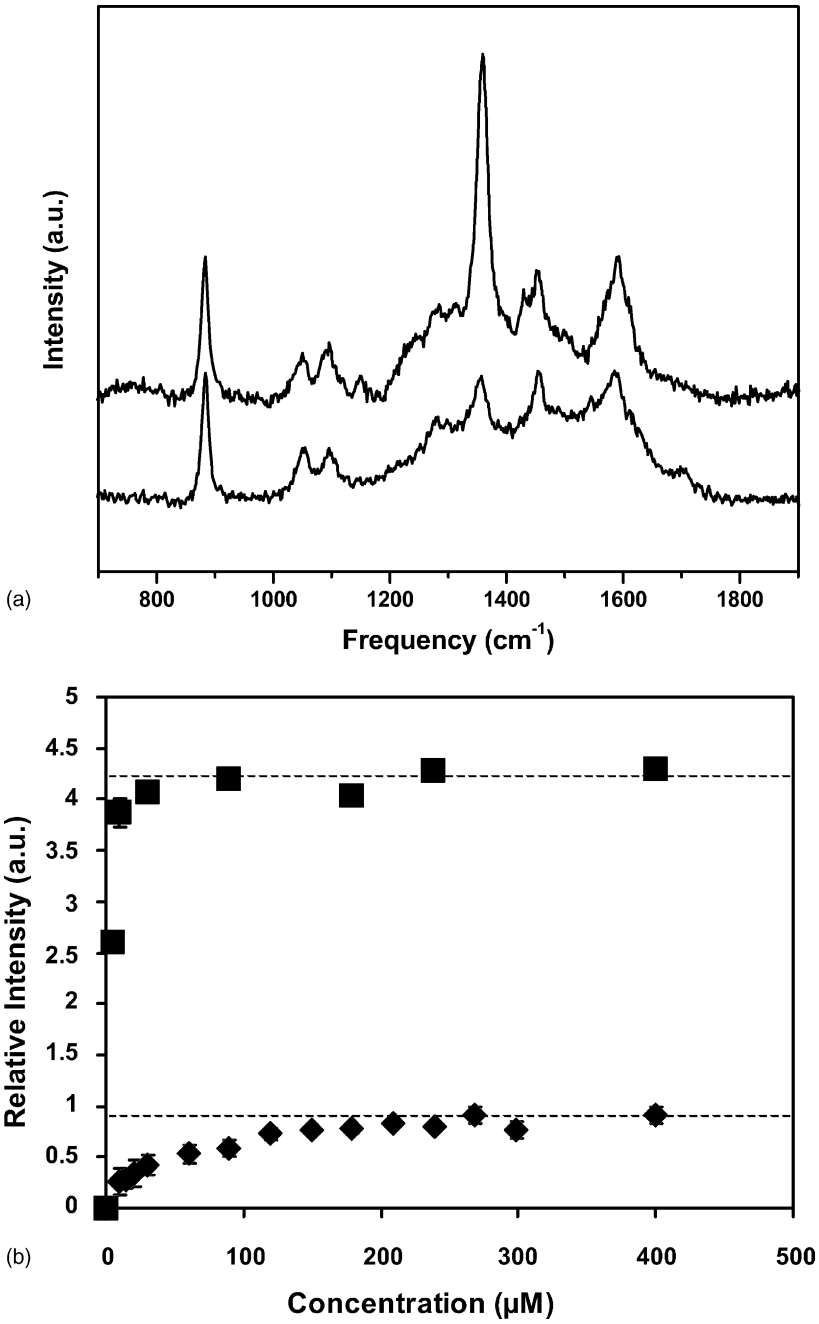

Fig. 8. (a) Typical in situ SER spectra obtained for platinum in a 0.120 mM cinchonidine in ethanol solution before (bottom) and after (top) introduction of solution-phase H_2. (b) Relative intensity of the 1357 cm^{-1} in-plane ring stretching vibration plotted as a function of liquid-phase cinchonidine concentration in ethanol in the presence of hydrogen (squares). The intensity scale is normalized to the maximum intensity obtained at the highest concentrations in the absence of hydrogen (diamonds).

peaks were observed is not surprising, since the detected SERS bands arise predominantly from the aromatic group, which remains unaltered between the two species. Comparison with cinchonidine adsorption at similar concentrations reveals that the main SERS peak for DHCD at 1357 cm^{-1} is already largely enhanced upon adsorption without H_2 present. While the presence of hydrogen in solution results in an increase in the intensity of the 1357 cm^{-1} peak, the effect is considerably less pronounced than for cinchonidine. For example, at similar concentrations of the two modifiers in solution, the increase in this peak is around a factor of 4.5 for cinchonidine (cf. Fig. 8b) versus 2 for DHCD. It thus appears likely that a large portion of the changes observed for adsorbed cinchonidine in the presence of hydrogen are a result of a conversion to DHCD on the surface. Another similarity between DHCD and H_2-exposed cinchonidine is the prominent appearance of the broad C-H out-of-plane mode at 784 cm^{-1} in both cases. This corresponds to a decrease

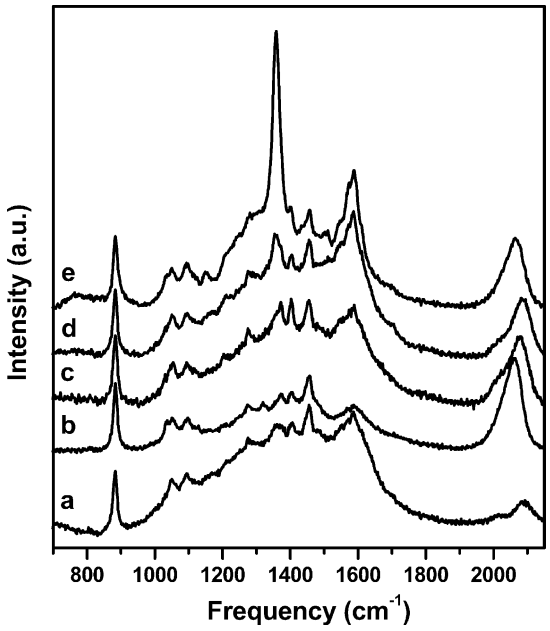

Fig. 9. Sequential in situ SER spectra obtained for: (a) platinum in ethanol, (b) after saturating with H_2, (c) after purging with He, (d) after introduction of 0.240 mM cinchonidine, and (e) after saturating with H_2 once again. See text for further details.

in the in-plane to out-of-plane ratio discussed earlier, and suggests a flatter orientation on the surface. The increase in the SERS intensity of the 1357 cm^{-1} band can thus be attributed in large part to increased π-bonding of the aromatic ring with the Pt surface.

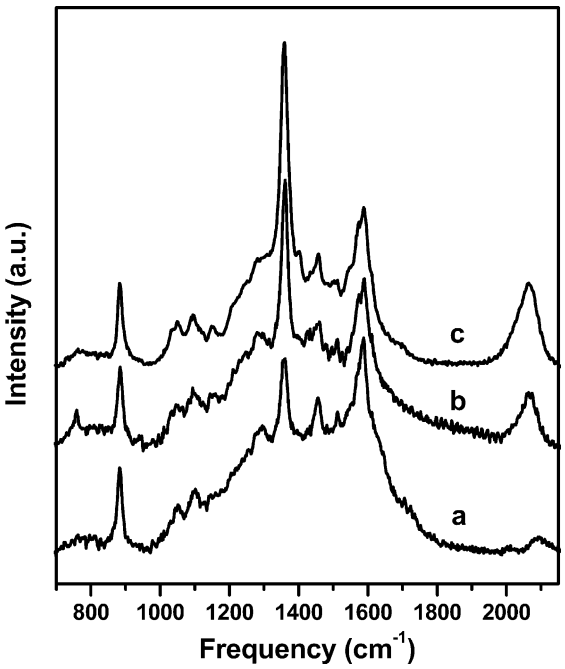

Fig. 10. Typical in situ SER spectra obtained for platinum in 0.240 mM 10,11-dihydrocinchonidine in ethanol: (a) before and (b) after introduction of solution-phase H_2. The SER Spectrum (c) of Pt in an H_2-saturated 0.240 mM cinchonidine in ethanol solution is provided for comparison.

Another possibility that must be considered is the presence of dissolved O_2 in the ethanol. Such solution-phase O_2 (and perhaps surface PtO_x) can play an important role in the adsorption of the modifier. For example, a recent RAIRS study by Ma et al. demonstrated that the presence of O_2 in cinchonidine/CCl_4 solutions greatly inhibits the adsorption of cinchonidine on polycrystalline Pt [16]. However, treatment with hydrogen resulted in enhanced adsorption, which was attributed to a reduction of the catalyst surface. In contrast to those results, the present findings in ethanol suggest that dissolved oxygen is not inhibiting cinchonidine adsorption to a large extent. Indeed, Raman measurements of cinchonidine adsorption in O_2-saturated ethanol (data not shown) revealed a negligible effect of this species on modifier adsorption behavior.

Kinetic studies of cinchonidine hydrogenation on Pt/Al_2O_3 suggest that DHCD is very strongly adsorbed on platinum, to the exclusion of cinchonidine and other more extensively hydrogenated species in solution [60]. This was indicated by the observation that once even a small amount of DHCD was formed in solution, the hydrogenation rate became zero order with respect to the alkaloid concentration in solution. The finding was consistent with the Pt surface being saturated with DHCD over a wide range of liquid-phase concentrations. Such saturation behavior is in harmony with the present observations, in that the coverage of hydrogenated cinchonidine is largely independent of liquid-phase cinchonidine concentration over a wide range of concentrations (cf. Fig. 8).

Another possibility for the H_2-induced changes that was considered involved the α-quinolyl species on the surface. The addition of H atoms onto the surface might be expected to drive hydrogenation of the aromatic ring back to cinchonidine. Ferri and Bürgi [12] observed such behavior in their ATR-IR investigation of this system. However, analysis of our data shows no significant change in the absolute intensity of the 1543 cm^{-1} α-quinolyl feature upon addition of hydrogen. This suggests that the surface coverage of this species remains largely unchanged, at least within the time resolution of our measurement. Furthermore, in the event of any conversion back to cinchonidine, further hydrogenation to DHCD would be expected under these conditions as described above.

4. Conclusions

Surface enhanced Raman spectroscopy has been utilized to probe the adsorption of the chiral modifier cinchonidine on polycrystalline platinum. Surfaces were prepared by electrodeposition of ultrathin platinum films onto roughened gold, which provided stable and intense SERS activity for performing these studies. The vibrational properties of adsorbed cinchonidine on platinum in ethanol solutions at 25 °C have been probed in situ. Based on the appearance and trends in the strong ring breathing mode at 1357 cm^{-1},

the modifier is strongly and irreversibly adsorbed through the quinoline portion of cinchonidine by π-bonding with the Pt surface. Furthermore, analysis of both in-plane and out-of-plane vibrations suggests that the cinchonidine is tilted with respect to the platinum surface. The degree of tilt appears to increase as concentration increases over the range of cinchonidine liquid-phase concentrations examined here (0.030–1.2 mM). The presence of an H-abstracted α-quinolyl species is also tentatively suggested by the appearance of a downshifted C=C stretching band not associated with cinchonidine. These findings are largely consistent with what has been observed previously using in situ infrared spectroscopy. Addition of hydrogen into the system results in enhanced Raman scattering from adsorbed cinchonidine. Comparisons with 10,11-dihydrocinchonidine adsorption in ethanol suggest that these H_2-induced changes likely result from hydrogenation of the vinyl group on cinchonidine. The data suggest a more flat orientation of this species, resulting from increased interaction of the aromatic ring structure with the surface. The results are consistent with kinetic studies of cinchonidine hydrogenation, which have implied stronger adsorption of 10,11-dihydrocinchonidine as compared with cinchonidine. Further SERS investigations of this important catalytic system are currently underway in our laboratory, focusing on both temperature effects and co-adsorption of cinchonidine with typical reactants (e.g., ethyl pyruvate, pyruvaldehyde dimethyl acetal).

Acknowledgements

This work was funded by the American Chemical Society Petroleum Research Fund (PRF) under ACS-PRF#35610-G5 and by the South Carolina Commission on Higher Education.

References

[1] A. Baiker, J. Mol. Catal. A: Chem. 115 (1997) 473–493.
[2] P.B. Wells, A.G. Wilkinson, Top. Catal. 5 (1998) 39–50.
[3] R.L. Augustine, K.T. Setrak, L.K. Doyle, Tetrahedron: Asymmetry 4 (1993) 1803.
[4] J.L. Margitfalvi, E. Tálas, E. Tfirst, C.V. Kumar, A. Gergely, Appl. Catal. A: Gen. 191 (2000) 177.
[5] H.-U. Blaser, H.-P. Jalett, M. Garland, M. Studer, H. Thies, A. Wirth-Tijana, J. Catal. 173 (1998) 282.
[6] J. Wang, Y.-K. Sun, C. LeBlond, R.N. Landau, D.G. Blackmond, J. Catal. 161 (1996) 752.
[7] Y.-K. Sun, J. Wang, C. LeBlond, R.N. Landau, D.G. Blackmond, J. Catal. 161 (1996) 759.
[8] C. LeBlond, J. Wang, A.T. Andrews, Y.-K. Sun, Top. Catal. 13 (2000) 169.
[9] A.F. Carley, M.K. Rajumon, M.W. Roberts, P.B. Wells, J. Chem. Soc., Faraday Trans. 91 (1995) 2167.
[10] J.M. Bonello, R.M. Lambert, Surf. Sci. 498 (2002) 212.
[11] D. Ferri, T. Bürgi, A. Baiker, J. Chem. Soc., Chem. Commun. (2001) 1172.
[12] D. Ferri, T. Bürgi, J. Am. Chem. Soc. 123 (2001) 12074.
[13] D. Ferri, T. Bürgi, A. Baiker, J. Catal. 210 (2002) 160.
[14] J. Kubota, F. Zaera, J. Am. Chem. Soc. 123 (2001) 11115.
[15] J. Kubota, Z. Ma, F. Zaera, Langmuir 19 (2003) 3371.
[16] Z. Ma, J. Kubota, F. Zaera, J. Catal. 219 (2003) 404.
[17] W. Chu, R.J. LeBlanc, C.T. Williams, Catal. Commun. 3 (2002) 547.
[18] S. Zou, M.J. Weaver, Anal. Chem. 70 (1998) 2387.
[19] M.J. Weaver, J. Raman Spectrosc. 33 (2002) 309.
[20] M.J. Weaver, Top. Catal. 8 (1999) 65.
[21] P. Gao, D. Gosztola, L.H. Leung, M.J. Weaver, J. Electroanal. Chem. 233 (1987) 211.
[22] A.J. Campion, P. Kambhampati, Chem. Soc. Rev. 27 (1998) 241.
[23] A. Kudelski, B. Pettinger, Chem. Phys. Lett. 321 (2000) 356.
[24] W. Chu, R.J. LeBlanc, C.T. Williams, J. Kubota, F. Zaera, J. Phys. Chem. B. 107 (2003) 14365.
[25] D. Lin-Vien, N. B. Colthup, W. G. Fateley, J. G. Grasselli, The Handbook of Infrared and Raman Characteristic Frequencies of Organic Molecules, Academic Press, San Diego, 1991.
[26] G. Socrates, Infrared and Raman Characteristic Group Frequencies (Tables and Charts), 3rd ed., Wiley, Chichester, 2001.
[27] A. Weselucha-Birczynska, K. Nakamoto, J. Raman Spectrosc. 27 (1996) 915.
[28] M.J. Frisch, G.W. Trucks, H.B. Schlegel, G.E. Scuseria, M.A. Robb, J.R. Cheeseman, V.G. Zakrzewski, J.A. Montgomery Jr., R.E. Stratmann, J.C. Burant, S. Dapprich, J.M. Millam, A.D. Daniels, K.N. Kudin, M.C. Strain, O. Farkas, J. Tomasi, V. Barone, M. Cossi, R. Cammi, B. Mennucci, C. Pomelli, C. Adamo, S. Clifford, J. Ochterski, G.A. Petersson, P.Y. Ayala, Q. Cui, K. Morokuma, D.K. Malick, A.D. Rabuck, K. Raghavachari, J.B. Foresman, J. Cioslowski, J.V. Ortiz, A.G. Baboul, B.B. Stefanov, G. Liu, A. Liashenko, P. Piskorz, I. Komaromi, R. Gomperts, R.L. Martin, D.J. Fox, T. Keith, M.A. Al-Laham, C.Y. Peng, A. Nanayakkara, M. Challacombe, P.M.W. Gill, B. Johnson, W. Chen, M.W. Wong, J.L. Andres, C. Gonzalez, M. Head-Gordon, E.S. Replogle, and J.A. Pople, Gaussian 98, Revision A.9, Gaussian, Inc., Pittsburgh, PA, 1998.
[29] B.M. Bode, M.S. Gordon, J. Mol. Graph. Mod. 16 (1999) 133.
[30] B.J. Oleksyn, Acta Cryst. B38 (1982) 1832.
[31] J.F. Margitfalvi, E. Tfirst, J. Mol. Catal. A 139 (1999) 81.
[32] A.D. Becke, J. Chem. Phys. 98 (1993) 5648.
[33] J.P. Perdew, Y. Wang, Phys. Rev. B 45 (1992) 13244.
[34] J.P. Perdew, J.A. Chevary, S.H. Vosko, K.A. Jackson, M.R. Pederson, D.J. Singh, C. Fiolhais, Phys. Rev. B 46 (1992) 6671.
[35] P.J. Hay, W.R. Wadt, J. Chem. Phys. 82 (1985) 270.
[36] W.R. Wadt, P.J. Hay, J. Chem. Phys. 82 (1985) 284.
[37] P.J. Hay, W.R. Wadt, J. Chem. Phys. 82 (1985) 299.
[38] A.P. Scott, L. Radom, J. Phys. Chem. 100 (1996) 16502.
[39] M.D. Halls, J. Velkovski, H.B. Schlegel, Theor. Chem. Acc. 105 (2001) 413.
[40] M.D. Halls, H.B. Schlegel, J. Chem. Phys. 111 (1999) 8819.
[41] M.D. Halls, H.B. Schlegel, J. Chem. Phys. 109 (1998) 10587.
[42] M.A. Palafox, Int. J. Quantum Chem. 77 (2000) 661.
[43] F. Tuinstra, J.L. Koenig, J. Chem. Phys. 53 (1970) 1126.
[44] A.G. Brolo, D.E. Irish, G. Szymanski, J. Lipkowski, Langmuir 14 (1998) 517.
[45] W.B. Lacy, L.G. Olson, J.M. Harris, Anal. Chem. 71 (1999) 2564.
[46] J.A. Creighton, in: R.J.H. Clark, R.E. Hester (Eds.), Spectroscopy of Surfaces, Wiley, 1988, p. 37.
[47] J. Chowdhury, M. Ghosh, T.N. Misra, Spectrochim. Acta A 56 (2000) 2107.
[48] K. Zawada, J. Bukowska, Surf. Sci. 507–510 (2002) 34.
[49] K. Zawada, J. Bukowska, J. Mol. Struct. 555 (2000) 425.
[50] V.H. Grassian, E.L. Muertterties, J. Phys. Chem. 90 (1986) 5900.
[51] S. Haq, D.A. King, J. Phys. Chem. 100 (1996) 16957.
[52] W.B. Cai, C.X. She, B. Ren, J.L. Yao, Z.W. Tian, Z.Q. Tian, J. Chem. Soc., Faraday Trans. 94 (1998) 3127.
[53] P. Cao, R. Gu, B. Ren, Z.Q. Tian, Chem. Phys. Lett. 366 (2002) 440.
[54] M. Garland, H.-U. Blaser, J. Am. Chem. Soc. 112 (1990) 7048.

[55] G.A. Attard, J.E. Gillies, C.A. Harris, D.J. Jenkins, P. Johnston, M.A. Price, D.J. Watson, P.B. Wells, Appl. Catal. A: Gen. 222 (2001) 393.
[56] C. LeBlond, J. Wang, A.T. Andrews, Y.-K. Sun, Top. Catal. 13 (2000) 169.
[57] B. Ren, X.XuX.Q. Li, W.B. Cai, Z.Q. Tian, Surf. Sci. 428 (1999) 157.
[58] A. Peremans, A. Tadjeddine, J. Chem. Phys. 103 (1995) 7197.
[59] A. Tadjeddine, A. Peremans, J. Electroanal. Chem. 409 (1996) 115.
[60] C. LeBlond, J. Wang, J. Liu, A.T. Andrews, Y.K. Sun, J. Am. Chem. Soc. 121 (1999) 4920.
[61] J. Chowdhury, M. Ghosh, T.N. Misra, Spectrochim. Acta A 56 (2000) 2107.
[62] M. Bolboaca, K. Kiefer, J. Popp, J. Raman Spectrosc. 33 (2002) 207.
[63] A.R. Katritzky, R.A. Jones, J. Chem. Soc. (1960) 2942.
[64] A. Weselucha-Birczynska, K. Nakamoto, J. Raman Spectrosc. 27 (1996) 915.